

Phase-Segregation-Induced Self-Assembly of Anisotropic MFI Microbuilding Blocks into Compact and Highly *b*-Oriented Monolayers

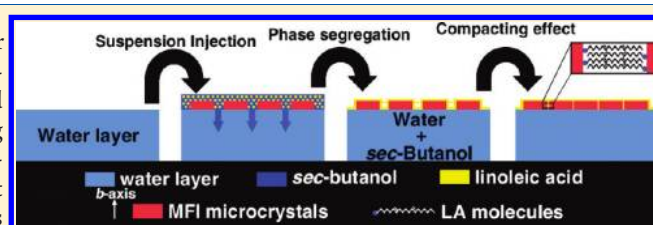
Yi Liu,^{†,‡} Yanshuo Li,[†] and Weishen Yang^{*,†}

[†]State Key Laboratory of Catalysis, Dalian Institute of Chemical Physics, Chinese Academy of Sciences, Dalian 116023, People's Republic of China

[‡]Graduate School of Chinese Academy of Sciences, Beijing 100039, People's Republic of China

S Supporting Information

ABSTRACT: A compact and highly *b*-oriented MFI monolayer was fabricated with a novel phase-segregation-induced self-assembly method. When MFI microcrystals were dispersed uniformly in an appropriate dispersant (*sec*-butanol) containing a trace amount of binding agent (linoleic acid), these microbuilding blocks were spontaneously self-assembled into a compact monolayer at an air–liquid interface. In particular, it was observed that the binding agent took effect only after being phase-segregated from the aqueous solution. The influence of the kind of dispersants and binding agents on the final morphology of the as-prepared MFI monolayers was discussed. On the basis of these results, a mechanism was proposed to elucidate the driving force for the compact and oriented assembly of these MFI building blocks at the air–water interface.



1. INTRODUCTION

The self-assembly of nanoparticles (NPs) into ordered two-dimensional (2D) layers has attracted great research interest because of its emerging application in advanced optical, electronic, magnetic, and sensing devices.¹ During the last few decades, a variety of approaches, such as drying-mediated assembly,² template-assisted assembly,³ and lithography,⁴ have been developed for the 2D organization of NPs at the surface and interface. Some extensive reviews have been published summarizing the new advances in this field.^{5,6} The 2D assembly of micrometer-sized building blocks, however, is still not explored to a large extent, although the ability to organize them will make materials chemistry flourish.⁷

Zeolite particles are ideal model microbuilding blocks for 2D assembly because of not only their ease in fabrication but also their inherent highly regular sub-nanometer-sized pore architectures, which may bring new features when being assembled into ordered 2D layers. In the recent years, great progress has been made in fabricating highly regular zeolite layers (unique orientation and high monolayer coverage) and their promising applications as high-performance molecular sieve membranes,^{8–15} anisotropic photoluminescence generators,¹⁶ light-harvesting systems,¹⁷ optical devices,^{18–20} selective sensors^{21–23} etc. have also been extensively explored.

Initiating from the 1990s, many approaches have been developed in an attempt to organize well-faceted zeolite particles (such as anisotropic MFI microcrystals) into highly oriented layers. By employing *in situ* growth, Yan et al. organized regular MFI nanocrystals grown from the precursor solution into a

highly *b*-oriented MFI monolayer on a smooth stainless-steel plate.²⁴ The key point to the successful orientation manipulation relies on the fine tuning of the synthetic composition and warranting smooth surface morphology of the substrate. Tsapatis et al. developed a convective assembly method to organize hexagonal ZSM-2 nanocrystals on a glass substrate.²⁵ Both out-of-plane and in-plane preferred orientations of these particles could be obtained in local areas, and interesting micrometer-sized regularly alternating stripes composed of particle deposits were also formed. The Langmuir–Blodgett (LB) approach is one of the most useful methods for the fabrication of monomolecular layers, and Doyle et al. recently reported that a homogeneous monolayer of nanosized silicalite-1 could be deposited on a silicon substrate using this technique.²⁶ This method was also tried in an attempt to organize micrometer-sized anisotropic MFI zeolite assemblies; however, the sedimentation of zeolite microcrystals during the transfer process could not be completely prevented, and both the continuity and degree of orientation of the films obtained were unsatisfactory.²⁷ Zhang et al. successfully fabricated *b*-oriented MFI monolayers on a polyvinyl alcohol (PVA)-modified α -Al₂O₃ substrate. A high degree of coverage (DOC) could be obtained with both sonication-assisted and manual assembly methods.²⁸ Yoon et al. developed a versatile method for depositing oriented zeolite monolayers by assembling zeolite microcrystals using organic

Received: December 5, 2010

Revised: January 21, 2011

Published: February 18, 2011

linkers.⁷ A wide variety of well-known chemical principles, such as covalent linkage,²⁹ ionic bonding,³⁰ and hydrogen bonding,³¹ could be exploited in this method. Moreover, on the basis of this viable seed-deposition method, a defect-free and highly *b*-oriented MFI membrane was successfully fabricated in Tsapatsis's group and exhibited excellent molecular-sieving properties in the separation of *p*-/*o*-xylene vapors.⁸

To summarize, the past few decades had witnessed great progress in fabricating highly oriented zeolite layers. However, a more facile and convenient method was still urgently required. With a MFI-type zeolite as model building blocks, recently, we invented an interface-aided method for the fabrication of highly *b*-oriented MFI monolayers on various substrates.³² Briefly, the substrate was precoated with a water layer, on which zeolite suspension (MFI microcrystals evenly dispersed in *sec*-butanol) was subsequently injected. Consequently, the MFI building blocks spontaneously self-assembled into a *b*-oriented monolayer at the air–water interface. With controlled evaporation of the liquid layer, the MFI monolayer was finally deposited onto the substrate. Here, in this work, we further improved the compactness of the MFI monolayer by introducing a trace amount of linoleic acid in the MFI-containing *sec*-butanol suspension before the injection, which was very beneficial for various practical applications (this work had been very briefly introduced in our previous work³³). Moreover, we also explored the influence of various preparative factors on the final microstructures of as-prepared MFI monolayers in more detail and put forward a phase-segregation-induced self-assembly mechanism to elucidate the exact formation process of this high-quality MFI monolayer.

2. MATERIALS AND METHODS

2.1. Synthesis of MFI Microcrystals. MFI (silcalite-1) microcrystals were synthesized according to a well-documented procedure,⁸ but with slight modification. For a typical synthesis, 7.626 g of tetrapropylammonium hydroxide (TPAOH) (20 wt %, Aldrich) and 7.5 g of tetraethyl orthosilicate (TEOS) (98%, Kermal) were mixed with 60 g of deionized (DDI) water. The mixture was further aged at room temperature for 24 h, then transferred to a Teflon-lined vessel, and placed in an oil bath with stirring. The temperature was maintained at 130 °C for 12 h, and the vessel was then removed from the oil bath and cooled to room temperature. The products were centrifuged at 6000 revolutions/min, washed 3 times with DDI water, and air-dried at 50 °C in an oven overnight.

2.2. Substrate Pretreatment. Before the deposition of MFI microbuilding blocks, a glass substrate (2 × 2 cm) was washed with DDI water, immersed in piranha solution (H₂SO₄/H₂O₂ = 2:1, v/v), and hydrothermally treated at 90 °C for 1 h to remove organic impurities. After that, it was washed with copious DDI water and stored in pure ethanol. Before use, it was dried with a hair drier.

2.3. *b*-Oriented Deposition of the MFI Layer. For the preparation of an alcohol-modified zeolite suspension, 0.02 g of MFI microcrystals were added to 5 mL of selected dispersant containing a trace amount of pre-added binding agent. Typically, 0.02 g of MFI microcrystals was mixed with 5 mL of *sec*-butanol (dispersant) and 1 μ L of linoleic acid (binding agent). By calculation, the number concentration of MFI particles in the suspension was 2.2×10^9 /mL. After vigorous stirring in a cone-shaped bottle at room temperature for more than 6 days, they were ready to be directly used in the subsequent experiment. For convenience, the addition amount of binding agent to the MFI suspension was defined as V_b , and $V_b = 1 \mu\text{L}$, if not specified otherwise.

The self-assembly process was conducted at 25 °C and 60% relative humidity (RH). Initially, a precleaned glass plate (2 × 2 cm) was placed

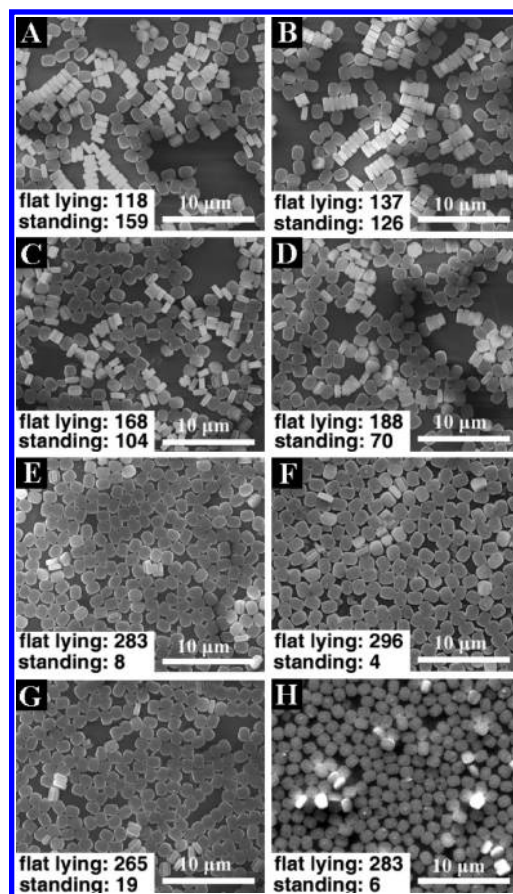


Figure 1. SEM images of MFI monolayers assembled using different dispersants: (A) methanol, (B) ethanol, (C) *n*-propanol, (D) *iso*-propanol, (E) *tert*-butanol, (F) *sec*-butanol (86.8%), (G) *iso*-butanol, and (H) *n*-butanol. $V = 75 \mu\text{L}$ for all kinds of suspensions, except *n*-butanol ($V = 10 \mu\text{L}$ for *n*-butanol). Note that the area of the substrate is $408.5 \mu\text{m}^2$ for all samples in the figure.

onto a horizontal plane. The substrate was then precoated with a water layer (0.8 mL), on which zeolite suspension was subsequently injected using an automatic injector (TJ-1A, Baoding Longer Precision Pump Co., Ltd.) at the speed of $2 \mu\text{L min}^{-1}$ until a continuous MFI monolayer was formed at the air–water interface. With controlled evaporation of the liquid layer, the as-prepared MFI layer was finally anchored to the substrate. In theory, 100 μL of alcohol suspension was required to achieve a full coverage of MFI microbuilding blocks on the substrate. However, the actual volume of suspension injected to the water layer was different under various conditions. Here, we define V as the volume of suspension that was injected to the water layer.

2.4. X-ray Diffraction (XRD), Scanning Electron Microscopy (SEM), and Attenuated Total Reflectance Infrared (ATR–IR) Spectroscopy Characterizations. Morphologies of the MFI seed monolayer and/or films were observed by SEM (Quanta 200 FEG, FEI Co., 30 kV). XRD patterns were recorded on Rigaku D/MAX 2500/PC instrument using Cu K α radiation ($\lambda = 0.154 \text{ nm}$ at 40 kV and 200 mA). The ATR–IR spectra of MFI microcrystals and/or monolayers were recorded on a Nicolet 6700 ATR–IR spectrometer. The 64 scans were collected at a resolution of 4 cm^{-1} .

3. RESULTS AND DISCUSSION

3.1. Selection of an Appropriate Dispersant. In a recent work, Doyle et al. prepared spin-coated silicalite-1 monolayers

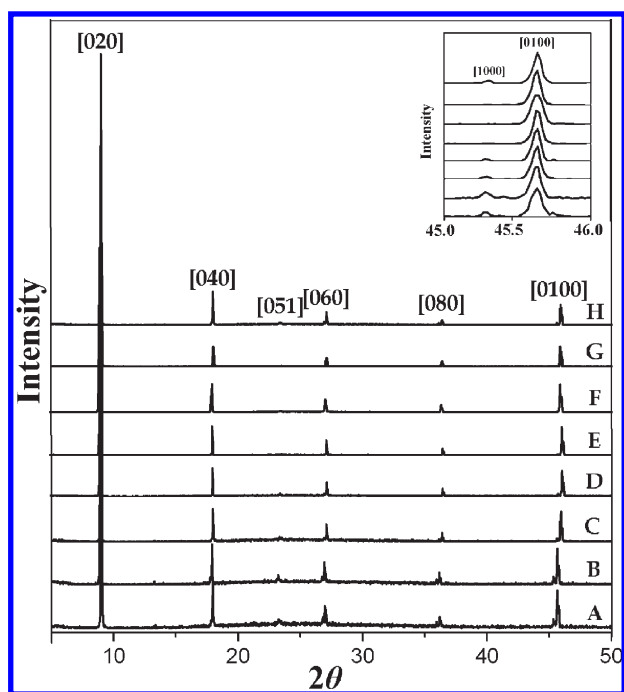


Figure 2. XRD patterns of MFI monolayers assembled using different dispersants: (A) methanol, (B) ethanol, (C) *n*-propanol, (D) *iso*-propanol, (E) *tert*-butanol, (F) *sec*-butanol, (G) *iso*-butanol, and (H) *n*-butanol. (Inset) Magnified XRD patterns for MFI monolayers with a 2θ angle between 45° and 46° .

with different alcohol dispersants, and their diverse morphologies were also attributed to the different hydrophobicity of the alcohol-decorated silicalite-1 crystals.³⁴ By analogy, here, we deduced that the hydrophobicity of alcohols might be an important factor influencing the final microstructures of the as-prepared MFI monolayer and should be explored further. Many experimental results also revealed that the hydrophobicity of silica materials could be increased to different extents by surface modification of alcohols with different chain length and molecular structure.^{35,36} Without the addition of any binding agents, here, various alcohols with different molecular structure and, thus, possessing different hydrophobicity, including methanol, ethanol, *n*-propanol, *iso*-propanol, *tert*-butanol, *sec*-butanol, *iso*-butanol, and *n*-butanol, were used as dispersants to investigate their roles in the self-assembly process. The as-prepared zeolite monolayers were then subjected to SEM and XRD characterization (Figures 1 and 2). To make a preliminary comparison of the degree of preferred *b* orientation of as-prepared MFI layers, the number of flat lying and standing MFI microbuilding blocks was also determined by the image analysis method (shown in insets of Figure 1). With methanol or ethanol as dispersants, the MFI monolayers exhibited similar morphology. Some of the MFI particles tended to co-align along their *b* axis and form stack assemblies, whereas others were individually arranged with their *b* axis perpendicular to the substrate (panels A and B of Figure 1). Stacks of the MFI microcrystals along their *b* axis were also observed when *n*-propanol or *iso*-propanol were chosen as dispersants (panels C and D of Figure 1); however, more of the particles tended to orient with their *b* axis perpendicular to the substrate, and the crystal stacking was not as serious as for the methanol or ethanol dispersant. For *tert*-butanol, *sec*-butanol, or *iso*-butanol, nearly all

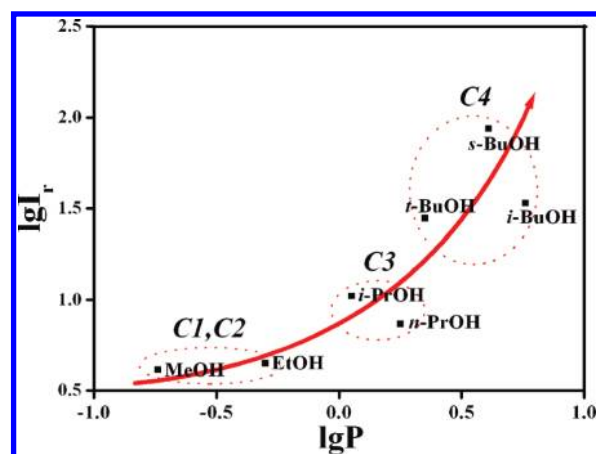


Figure 3. Log I_r values for zeolite monolayers versus the log P values of various aliphatic alcohols used as dispersants.

of the zeolite particles were anchored to the substrate with their *b* axis perpendicular to the substrate (panels E–G of Figure 1). The only discrepancy was that MFI microbuilding blocks were more densely packed for *sec*-butanol dispersant, and there was more open space for *tert*-butanol and *iso*-butanol. *n*-Butanol also induced the formation of highly *b*-oriented zeolite monolayers in local areas, similar to *sec*-butanol (Figure 1H); however, there were also large bare areas not covered by zeolite particles, and a few MFI microcrystals were stacked with no preferential orientation in some areas on the substrate (see SI-1 in the Supporting Information).

The SEM and XRD results confirmed that MFI particles mainly showed preferential *a* and *b* orientations on the substrate. As a measure of the degree of preferential *b* orientation over *a* orientation of the zeolite monolayers, we define $I_r = I_{[0\ 10\ 0]}/I_{[10\ 0\ 0]}$, where $I_{[0\ 10\ 0]}$ and $I_{[10\ 0\ 0]}$ are the peak heights of the $[0\ 10\ 0]$ ($2\theta = 45.7^\circ$) and $[10\ 0\ 0]$ ($2\theta = 45.3^\circ$) peaks for MFI monolayers, respectively. The larger the I_r value, the greater the preferential *b* orientation of the zeolite monolayers. By calculation, we find that I_r generally increases in the order: methanol \approx ethanol $<$ *n*-propanol \approx *iso*-propanol $<$ *tert*-butanol \approx *iso*-butanol $<$ *sec*-butanol. Thus, *sec*-butanol-modified zeolite microcrystals exhibited the highest degree of *b* orientation, which would be selected as the standard dispersant in the following experiments. Furthermore, the DOC (defined as the percentage of the attached area of MFI crystals in the monolayer with respect to the area of total substrate) of MFI microcrystals on the substrate reached 86.8% with dispersant *sec*-butanol.

To quantitatively define the degree of hydrophobicity of dispersants used here, we use the hydrophobic parameter $\log P$ [$\log P = \log(C_{n\text{-octanol}}/C_{\text{water}})$, where $C_{n\text{-octanol}}/C_{\text{water}}$ denotes the equilibrium ratio of a chemical in *n*-octanol and water; the values for different dispersants can be found elsewhere³⁷]. The $\log P$ value for different dispersants increased in the order methanol $<$ ethanol $<$ *iso*-propanol $<$ *n*-propanol $<$ *tert*-butanol $<$ *sec*-butanol $<$ *iso*-butanol. Here, we verify the relationship between I_r values of zeolite monolayers and $\log P$ values of related dispersant by plotting the I_r – $\log P$ curve, and the results are shown in Figure 3. We find that, generally speaking, the I_r values have positive correlation with the $\log P$ values of the used dispersants and the number of carbon atoms in alcohol molecules. However, further investigation was needed to give a satisfactory interpretation of these experimental results.

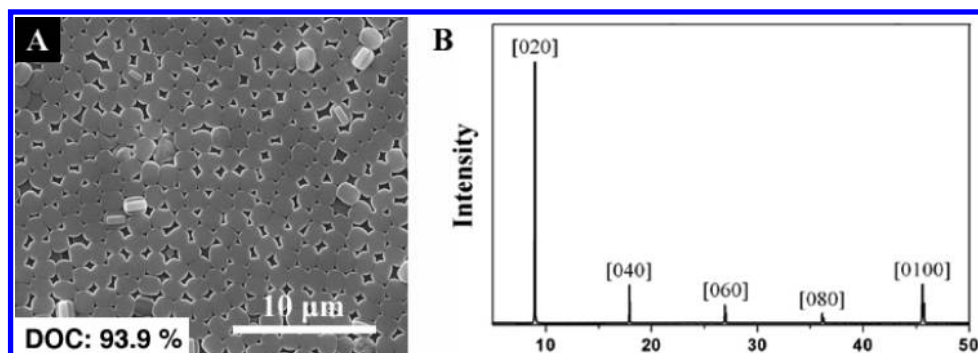


Figure 4. (A) SEM image of the as-prepared MFI monolayer with *sec*-butanol as the dispersant and linoleic acid as the binding agent ($V = 85 \mu\text{L}$) and (B) XRD pattern of the MFI monolayer.

3.2. Elucidation of the Mechanism for the Influence of Dispersant on Final Morphology. Surface modification with alcohol molecules can make MFI microcrystals more hydrophobic³⁸ and ensure that they all float at the air–water interface and spontaneously self-assemble into a monolayer (see SI-2 in the Supporting Information). Nevertheless, our experimental results showed that the quality, including the degree of coverage and orientation of assembled zeolite monolayers, is strongly related to the kind of alcohols used as dispersants (Figures 1 and 2). In theory, the morphological diversity of MFI layers was driven by their natural tendency to minimize the Gibbs free energy at the air–liquid interface. Originally, these anisotropic MFI building blocks tended to arrange with their *b* axis perpendicular to the air–water interface out of geometric and gravity effects. However, to minimize unfavorable interactions with the hydrophilic water layer, these alcohol-modified hydrophobic MFI microbuilding blocks would choose to attach to the air–water interface with their small facet and stack together with their large facets, thus forming chain-like structures along the *b* axis, as was shown in panels A and B of Figure 1 (methanol and ethanol as dispersants). Nevertheless, with increasing the number of carbon atoms in dispersant molecules (3 and/or 4 carbon atoms, shown in panels C–H of Figure 1), *b*-oriented stacking of these microcrystals became substantially alleviated; correspondingly, more of them tended to attach to the water layer with their largest facets. This experimental observation can be interpreted considering the steric hindrance effect of the alkyl groups. Similarly, alkyl-chain groups are often anchored onto the crystal surface to prevent nanoparticle agglomeration for the synthesis of nanocrystals.³⁹ The existence of the repulsive interaction between silanized micrometer-sized glass spheres was also confirmed during their self-assembly process by the LB technique.⁴⁰ Therefore, we deduced that, with the increment of the number of carbon atoms and the hydrophobicity ($\log P$) of alcohol molecules, the steric hindrance effect between alcohol-modified MFI microcrystals was also strengthened, which in turn had severely hampered the *b*-oriented stacking of MFI microbuilding blocks. Therefore, the *b*-oriented arrangement of MFI microcrystals gradually became dominant. However, further probing into this system was still necessary to achieve a more comprehensive understanding of this *b*-oriented self-assembly process.

3.3. Formation of More Compact MFI Monolayers. In most cases, the fabrication of zeolite monolayers, which are not only highly oriented but also very compact, is more favorable for practical applications. By analogy with the spontaneous self-

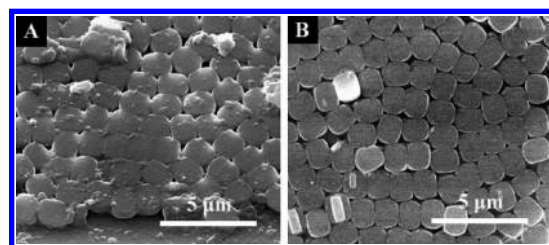


Figure 5. SEM images of the MFI monolayer obtained (A) before and (B) after calcinations.

assembly of surfactant-coated nanoparticles because of noncovalent interactions between long-chain alkyl groups anchored to the crystal surface,⁴¹ here, with *sec*-butanol as a standard dispersant, we further added a trace amount of linoleic acid to the MFI-containing suspension and expected that serve as a “binding agent” to facilitate the formation of a more compact MFI monolayer.

Following the same manufacturing procedure as shown above, the as-prepared MFI layer was subject to SEM characterization. Interestingly, it was shown that a very compact and uniform MFI monolayer was indeed formed (in comparison to Figure 1F), with each microcrystal anchored to the glass substrate with the largest facet (Figure 4A). In comparison to the one obtained without the addition of organic additives, the DOC of the substrate surface with MFI crystals has increased to 93.9%. XRD characterization (Figure 4B) further confirmed the strong *b* orientation, and the $[0\ k\ 0]$ diffraction peaks were dominant in the whole pattern.

3.4. Elucidation of the Mechanism of the Compacting Effect. As shown above, MFI building blocks were in contact with each other more closely when a trace amount of linoleic acid was added into the MFI-containing suspension. To elucidate the compact mechanism, the as-prepared MFI monolayer was further calcined and a detailed comparison between the sample before and after calcination was made. As shown in Figure 5A, for the uncalcined sample, void spaces between MFI building blocks were filled with unknown substances. After calcination, however, the filler that originally existed in the gaps of neighboring MFI microcrystals had completely disappeared (Figure 5B). Taking consideration of the fact that only MFI microcrystals, *sec*-butanol, linoleic acid, and water were present in the system and only linoleic acid can exist in the solid state at experimental conditions (25 °C) while decomposing when subjected to calcination, we deduced that the unidentified substances were linoleic acid.

Figure 6A showed the ATR-IR spectra of the as-prepared MFI monolayer. To facilitate the identification of functional groups on the outer surface of the MFI monolayer, the ATR-IR spectra of MFI microbuilding blocks obtained by the direct drying of linoleic-acid-containing *sec*-butanol suspension of MFI microcrystals were also recorded (Figure 6B). As observed in Figure 6, the appearance of stretching vibrations of O-H ($3200\text{--}3400\text{ cm}^{-1}$) groups, C-H ($-\text{CH}$, 2958, 2925, and 2854 cm^{-1} ; $=\text{CH}$, 3093 cm^{-1}) groups, and C=O (1714 cm^{-1}) groups clearly proved that linoleic acid molecules were still adsorbed on the outer surface of MFI monolayers even after the oriented deposition. In comparison to the ATR-IR spectra of pure linoleic acid and MFI monolayer prepared without the addition of binding agent (see SI-3 in the Supporting Information), we came to the conclusion that the unidentified substance adhering at the vicinity of MFI microbuilding blocks (Figure 6A) was linoleic acid.

On the basis of the above results, we put forward a phase-segregation-induced compacting mechanism to account for the assembly process. In this MFI-containing alcohol suspension, each component (MFI building blocks, *sec*-butanol, and linoleic acid) cherished different solubility in water. After being injected onto the water layer, MFI microcrystals were immediately separated from the aqueous suspension and floated at the

air-water interface because of their hydrophobicity discrepancy. Meanwhile, with the unceasing dissolution of the *sec*-butanol component (solubility = $12.5\text{ g}/100\text{ g}$ of H_2O) in water, linoleic acid (solubility = insoluble) was also segregated from water and formed the third phase. Moreover, through hydrogen-bonding interactions, linoleic acid molecules were spontaneously migrated and adhered to the outer surface of MFI microcrystals. Finally, because of the strong inherent cohesive forces originated from noncovalent interactions between long-chain alkyl groups of linoleic acid molecules adsorbed on the crystal surface, MFI building blocks were induced to spontaneously contact with each other more closely and firmly. This process was schematically illustrated in Figure 7 in detail.

The successful phase separation of the binding agent from the aqueous solution relies on its extremely low insolubility in water, which is the key step for the compact assembly of MFI microbuilding blocks. To further confirm the existence of phase separation during self-assembly, here, a series of carboxylic-acid-type surfactants with different alkyl tail chain lengths (alkyl chain of 3–24 carbons) and, thus, different solubility in water were used as binding agents. As shown in Figure 8, with acrylic acid (3 carbons; solubility = unlimited) and/or *trans*-3-hexenoic acid (6 carbons; solubility = slightly soluble) as binding agents (panels A and B of Figure 8), even though the V_b value had reached $100\text{ }\mu\text{L}$, the as-prepared MFI monolayers were still not compact enough (the DOC reached 87.8 and 85.7%, respectively), implying that surfactant molecules with short alkyl chain length were not suitable to be used as binding agents. However, once the chain length increased to 12 carbons (*cis*-5-dedecenoic acid; solubility = insoluble), the binding agent began to work. As shown in Figure 8C, a compact and *b*-oriented MFI monolayer formed when *cis*-5-dedecenoic acid was added to the suspension ($V_b = 3\text{ }\mu\text{L}$), with the DOC of 94.7%. However, there still existed some bare areas that MFI building blocks did not cover (see SI-4 in the Supporting Information). Similar microstructures were also observed when arachidonic acid (24 carbons) was used ($V_b = 1\text{ }\mu\text{L}$) as the binding agent (Figure 8D), with the DOC of 95.5%.

The morphological diversity of the as-prepared MFI monolayers can be rationally interpreted by taking into consideration the solubility discrepancy of these binding agents used in the experiment. If the alkyl chain was not long enough (less than 12 carbons), such as acrylic acid or *trans*-3-hexenoic acid, these molecules would be more prone to dissolve into the water layer because of their considerable solubility in water. Accordingly, a few of them may remain adsorbed on the surface of MFI microcrystals. As a result, the cohesive forces between MFI building blocks originating from the noncovalent interactions

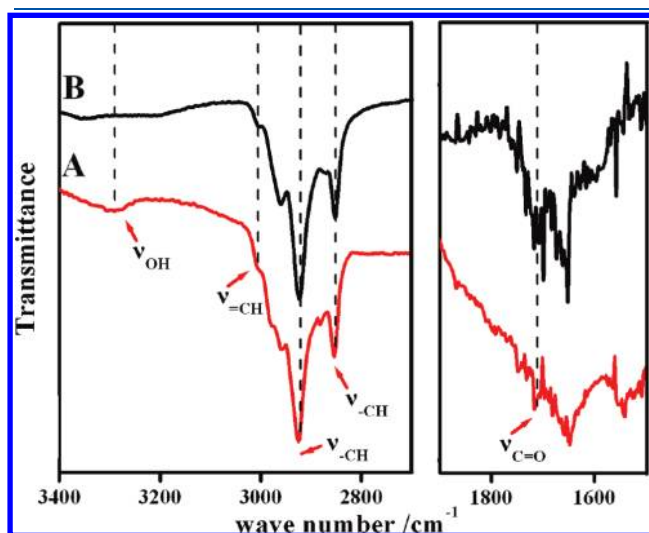


Figure 6. ATR-IR spectra of (A) as-prepared MFI monolayer obtained with *sec*-butanol as the dispersant and linoleic acid as the binding agent and (B) MFI microcrystals obtained by the direct drying of the linoleic-acid-containing *sec*-butanol suspension of MFI microcrystals.

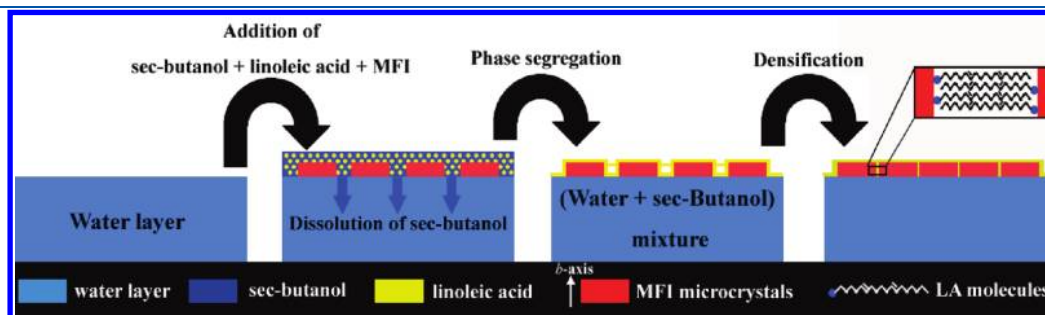


Figure 7. Schematic illustration of the process of phase-segregation-induced compact assembly of MFI microbuilding blocks at the air-water interface.

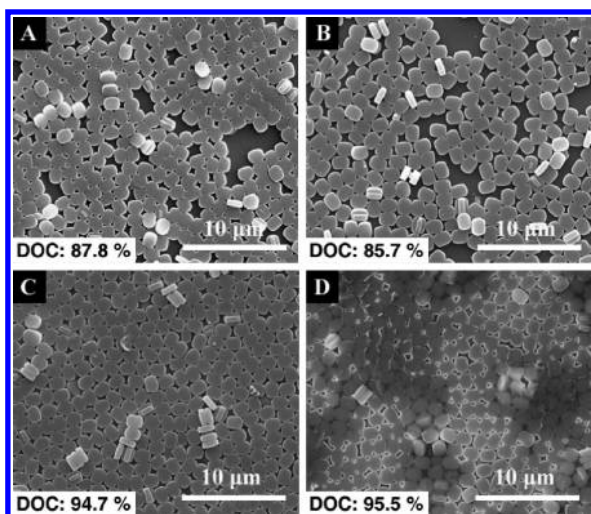


Figure 8. SEM images of MFI layers obtained with (A) acrylic acid ($V_b = 100 \mu\text{L}$; $V = 78 \mu\text{L}$), (B) *trans*-3-hexenoic acid ($V_b = 100 \mu\text{L}$; $V = 75 \mu\text{L}$), (C) *cis*-5-dedocenic acid ($V_b = 3 \mu\text{L}$; $V = 80 \mu\text{L}$), and (D) arachidonic acid ($V_b = 1 \mu\text{L}$; $V = 80 \mu\text{L}$) as binding agents. It should be noted that DOC is the abbreviation for “degree of coverage”, as shown in the main text.

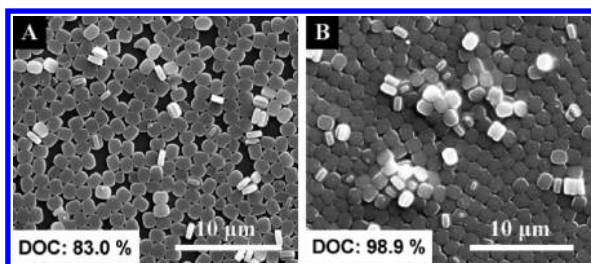


Figure 9. SEM images of MFI layers obtained with linoleic acid as binding agents. The addition amount was (A) $V_b = 0.5 \mu\text{L}$ and $V = 75 \mu\text{L}$ and (B) $V_b = 2 \mu\text{L}$ and $V = 85 \mu\text{L}$.

between long-chain alkyl groups were weak, and the compact arrangement of the MFI blocks at the air–liquid interface became unavailable. In contrast, once the alkyl tail chain of surfactant molecules became long enough (more than 12 carbons), phase separation took place because of its extremely low solubility in water and then the compacting effect took effect. The morphological evolution of the as-prepared MFI monolayers with the increase of the alkyl tail chain length of surfactant molecules vividly proved the key role of phase separation of the binding agent in the compact self-assembly of MFI microbuilding blocks.

3.5. Optimization of the Addition Amount of the Binding Agent. By trial and error, it was found that linoleic acid was the most effective binding agent facilitating the formation of a densely packed and highly *b*-oriented MFI monolayer (see SI-5 in the Supporting Information). Here, influence of its concentration in *sec*-butanol suspension on the microstructure of the as-prepared monolayer was investigated in detail. As shown in Figure 9, when the addition amount of linoleic acid was $0.5 \mu\text{L}$ ($V_b = 0.5 \mu\text{L}$), MFI microcrystals could only be deposited on the substrate with moderate compactness (DOC of 83.0%); however, once the addition amount reached $2 \mu\text{L}$ ($V_b = 2 \mu\text{L}$), an extremely compact MFI monolayer with quite narrow

intercrystalline gaps was formed (DOC of 98.9%). However, a few of the MFI microcrystals still exhibited an irregularly arrangement, probably because that excess amount of linoleic acid molecules was adsorbed on the crystal surface, which may lead to overly strong attractive interactions between some MFI building blocks, deteriorating the regularity. It is also very promising that defects on this extremely compact MFI layer can be eliminated by optimization of the manufacturing procedure and experimental parameters, which would be more favorable for practical applications.

4. CONCLUSION

To summarize, here, we developed a new approach to fabricate high-quality MFI monolayers. By trial and error, it was found that, by dispersing MFI microcrystals into appropriate dispersant (*sec*-butanol) and binding agent (linoleic acid), these microbuilding blocks were spontaneously self-assembled into a compact and highly *b*-oriented monolayer by being injected onto a water layer. The *sec*-butanol component mainly facilitated the *b*-oriented deposition of MFI microcrystals onto the water layer, while linoleic acid served as an efficient binding agent, rendering MFI microcrystals contact with each other more closely. A phase-segregation-induced self-assembly mechanism was proposed to illuminate the exact formation process of the high-quality MFI layer. Because of their solubility discrepancy in water, *sec*-butanol tended to dissolve in the water layer and, simultaneously, linoleic acid was separated from the dispersant and adhered onto the surface of MFI microbuilding blocks, which would greatly facilitate their compact arrangement, relying on the noncovalent interactions between long-chain alkyl groups. In future work, we will strive to further optimize the experimental conditions and seek out more suitable dispersant and binding agents to fabricate the MFI monolayer with more perfect and versatile microstructures.

■ ASSOCIATED CONTENT

Supporting Information. Detailed morphology of the MFI layer obtained with *n*-butanol as a dispersant (SI-1), MFI layer obtained without being subjected to alcohol modification (SI-2), ATR–IR spectra of pure linoleic acid and the MFI monolayer prepared without the addition of binding agent (SI-3), detailed morphologies of MFI monolayers obtained with *sec*-butanol as a dispersant and *cis*-5-dedocenic acid and/or arachidonic acid as binding agents (SI-4), and influence of different binding agents on the final morphologies of as-prepared MFI layers (SI-5). This material is available free of charge via the Internet at <http://pubs.acs.org>.

■ AUTHOR INFORMATION

Corresponding Author

*Telephone: +86-411-84379073. Fax: +86-411-84379073. E-mail: yangws@dicp.ac.cn.

■ ACKNOWLEDGMENT

This work was supported by the National Science Fund for Distinguished Young Scholars (20725313), the Dalian Institute of Chemical Physics (DICP) Independent Research Project (R201006), and the Ministry of Science and Technology of China (Grant 2003CB615802).

REFERENCES

- (1) Srivastava, S.; Kotov, N. A. *Soft Matter* **2009**, *5*, 1146–1156.
- (2) Bigioni, T. P.; Lin, X. M.; Nguyen, T. T.; Corwin, E. I.; Witten, T. A.; Jaeger, H. M. *Nat. Mater.* **2006**, *5*, 265–270.
- (3) Gao, H.; Gosvami, N. N.; Deng, J.; Tan, L. S.; Sander, M. S. *Langmuir* **2006**, *22*, 8078–8082.
- (4) Li, Y. F.; Zhang, J. H.; Zhu, S. J.; Dong, H. P.; Jia, F.; Wang, Z. H.; Tang, Y.; Zhang, L.; Zhang, S. Y.; Yang, B. *Langmuir* **2010**, *26*, 9842–9847.
- (5) Kinge, S.; Crego-Calama, M.; Reinhoudt, D. N. *ChemPhysChem* **2008**, *9*, 20–42.
- (6) Boker, A.; He, J.; Emrick, T.; Russell, T. P. *Soft Matter* **2007**, *3*, 1231–1248.
- (7) Yoon, K. B. *Acc. Chem. Res.* **2007**, *40*, 29–40.
- (8) Lai, Z. P.; Bonilla, G.; Diaz, L.; Nery, J. G.; Sujaoti, K.; Amat, M. A.; Kokkoli, E.; Terasaki, O.; Thompson, R. W.; Tsapatsis, M.; Vlachos, D. G. *Science* **2003**, *300*, 456–460.
- (9) Choi, J.; Jeong, H. K.; Snyder, M. A.; Stoeger, J. A.; Masel, R. L.; Tsapatsis, M. *Science* **2009**, *325*, 590–593.
- (10) Choi, J.; Tsapatsis, M. *J. Am. Chem. Soc.* **2010**, *132*, 448–449.
- (11) Veziri, C. M.; Palomino, M.; Karanikolos, G. N.; Corma, A.; Kanellopoulos, N. K.; Tsapatsis, M. *Chem. Mater.* **2010**, *22*, 1492–1502.
- (12) Karanikolos, G. N.; Wydra, J. W.; Stoeger, J. A.; Garcia, H.; Corma, A.; Tsapatsis, M. *Chem. Mater.* **2007**, *19*, 792–797.
- (13) Choi, J.; Ghosh, S.; Lai, Z. P.; Tsapatsis, M. *Angew. Chem., Int. Ed.* **2006**, *45*, 1154–1158.
- (14) Lai, Z. P.; Tsapatsis, M. *Ind. Eng. Chem. Res.* **2004**, *43*, 3000–3007.
- (15) Lee, I.; Jeong, H. K. *Microporous Mesoporous Mater.* **2011**10.1016/j.micromeso.2010.11.012.
- (16) Lee, J. S.; Lim, H.; Ha, K.; Cheong, H.; Yoon, K. B. *Angew. Chem., Int. Ed.* **2006**, *45*, 5288–5292.
- (17) Ruiz, A. Z.; Li, H.; Calzaferri, G. *Angew. Chem., Int. Ed.* **2006**, *45*, 5282–5287.
- (18) Kim, D.; Rhee, B. K.; Yoon, K. B. *J. Am. Chem. Soc.* **2004**, *126*, 673–682.
- (19) Kim, H. S.; Pham, T. T.; Yoon, K. B. *J. Am. Chem. Soc.* **2008**, *130*, 2134–2135.
- (20) Shu, G.; Liu, J. M.; Chiang, A. S. T.; Thompson, R. W. *Adv. Mater.* **2006**, *18*, 185–189.
- (21) Li, S.; Wang, X.; Beving, D.; Chen, Z. W.; Yan, Y. S. *J. Am. Chem. Soc.* **2004**, *126*, 4122–4123.
- (22) Gora, L.; Kuhn, J.; Baimpos, T.; Nikolakis, V.; Kapteijn, F.; Serwicka, E. M. *Analyst* **2009**, *134*, 2118–2122.
- (23) Zampieri, A.; Dubbe, A.; Schwieger, W.; Avhale, A.; Moos, R. *Microporous Mesoporous Mater.* **2008**, *111*, 530–535.
- (24) Wang, Z. B.; Yan, Y. S. *Chem. Mater.* **2001**, *13*, 1101–1107.
- (25) Lee, J. A.; Meng, L.; Norris, D. J.; Scriven, L. E.; Tsapatsis, M. *Langmuir* **2006**, *22*, 5217–5219.
- (26) Wang, Z.; Wee, L. K.; Mihailova, B.; Edler, K. J.; Doyle, A. M. *Chem. Mater.* **2007**, *19*, 5806–5808.
- (27) Morawetz, K.; Reiche, J.; Kamusewitz, H.; Kosmella, H.; Ries, R.; Noack, M.; Brehmer, L. *Colloids Surf., A* **2002**, *198–200*, 409–414.
- (28) Zhang, B. Q.; Zhou, M.; Liu, X. F. *Adv. Mater.* **2008**, *20*, 2183–2189.
- (29) Kulak, A.; Lee, Y. J.; Park, Y. S.; Yoon, K. B. *Angew. Chem., Int. Ed.* **2000**, *39*, 950–953.
- (30) Lee, G. S.; Lee, Y. J.; Yoon, K. B. *J. Am. Chem. Soc.* **2001**, *123*, 9769–9779.
- (31) Lee, J. S.; Kim, J. H.; Lee, Y. J.; Jeong, N. C.; Yoon, K. B. *Angew. Chem., Int. Ed.* **2007**, *46*, 3087–3090.
- (32) Liu, Y.; Li, Y. S.; Yang, W. S. *Chem. Commun.* **2009**, 1520–1522.
- (33) Liu, Y.; Li, Y. S.; Yang, W. S. *J. Am. Chem. Soc.* **2010**, *132*, 1768–1769.
- (34) Wee, L. H.; Tosheva, L.; Vasilev, C.; Doyle, A. M. *Microporous Mesoporous Mater.* **2007**, *103*, 296–301.
- (35) Hunter, T. N.; Wanless, E. J.; Jameson, G. J. *Colloids Surf., A* **2009**, *334*, 181–190.
- (36) Fuji, M.; Takei, T.; Watanabe, T.; Chikazawa, M. *Colloids Surf., A* **1999**, *154*, 13–24.
- (37) Log *P* values for the different alcohols used in the experiment can be obtained at <http://logkow.cisti.nrc.ca/logkow/>.
- (38) Cheng, C. H.; Bae, T. H.; McCool, B. A.; Chance, R. R.; Nair, S.; Jones, C. W. *J. Phys. Chem. C* **2008**, *112*, 3543–3551.
- (39) Prasad, B. L. V.; Stoeva, S. I.; Sorensen, C. M.; Klabunde, K. J. *Langmuir* **2002**, *18*, 7515–7520.
- (40) Hórvölgyi, Z.; Németh, S.; Fendler, J. H. *Langmuir* **1996**, *12*, 997–1004.
- (41) Wang, X.; Li, Y. D. *Chem. Commun.* **2007**, 2901–2910.